JACS
JOURNAL OF THE AMERICAN CHEMICAL SOCIETY
Article
pubs.acs.org/JACS

Optoelectronic Studies of Methylammonium Lead Iodide Perovskite Solar Cells with Mesoporous TiO_2: Separation of Electronic and Chemical Charge Storage, Understanding Two Recombination Lifetimes, and the Evolution of Band Offsets during *J*–*V* Hysteresis

Brian C. O'Regan,*[,†] Piers R. F. Barnes,[‡] Xiaoe Li,[†] Chunhung Law,[†] Emilio Palomares,[§,∥] and Jose M. Marin-Beloqui[§]

[†]Chemistry Department, Imperial College, 1 Exhibition Road, London SW7 2AZ, U.K.
[‡]Physics Department, Imperial College, 1 Exhibition Road, London SW7 2AZ, U.K.
[§]Institute of Chemical Research of Catalonia (ICIQ), Avda. Països Catalans,16, Tarragona E-43007, Spain
[∥]ICREA, Passeig Lluis Companys, 23, E-08010 Barcelona, Spain

Supporting Information

ABSTRACT: Methylammonium lead iodide (MAPI) cells of the design FTO/$sTiO_2$/$mpTiO_2$/MAPI/Spiro-OMeTAD/Au, where FTO is fluorine-doped tin oxide, $sTiO_2$ indicates solid-TiO_2, and $mpTiO_2$ is mesoporous TiO_2, are studied using transient photovoltage (TPV), differential capacitance, charge extraction, current interrupt, and chronophotoamperometry. We show that in $mpTiO_2$/MAPI cells there are two kinds of extractable charge stored under operation: a capacitive electronic charge (~0.2 μC/cm^2) and another, larger charge (40 μC/cm^2), possibly related to mobile ions. Transient photovoltage decays are strongly double exponential with two time constants that differ by a factor of ~5, independent of bias light intensity. The fast decay (~1 μs at 1 sun) is assigned to the predominant charge recombination pathway in the cell. We examine and reject the possibility that the fast decay is due to ferroelectric relaxation or to the bulk photovoltaic effect. Like many MAPI solar cells, the studied cells show significant *J*–*V* hysteresis. Capacitance vs open circuit voltage (V_{oc}) data indicate that the hysteresis involves a change in internal potential gradients, likely a shift in band offset at the TiO_2/MAPI interface. The TPV results show that the V_{oc} hysteresis is not due to a change in recombination rate constant. Calculation of recombination flux at V_{oc} suggests that the hysteresis is also not due to an increase in charge separation efficiency and that charge generation is not a function of applied bias. We also show that the *J*–*V* hysteresis is not a light driven effect but is caused by exposure to electrical bias, light or dark.

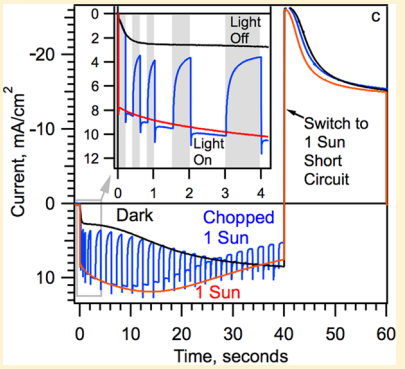

INTRODUCTION

Photovoltaic cells constructed from methylammonium lead iodide, $CH_3NH_3PbI_3$ (MAPI), and related materials have generated much interest in the last 2 years. The energy conversion efficiency has been increasing very rapidly since their first description at 3.8%[1] to the current reports ranging from 15% to 18%.[2−4] At the same time, there is much debate about the optoelectronic mechanisms that allow this low temperature material to deliver such high efficiencies. Debate concerns the possible roles of crystal size, stoichiometry, defects, and ferroelectric domains. There is debate about where in the cell the voltage is generated, the type of recombination, importance of traps, doping levels, and more. There is also debate about how to correctly measure the recombination and transport times, the charge density, and even the correct measurement of efficiency.[5−17] The debate about characterization centers on the interpretation of various time constants that can be measured by optical and electrical means. These time constants range from <1 to >100 μs. It is not yet agreed which time constants correspond to major recombination and transport pathways. We believe we can correctly assign some of these times based on the data presented herein. The debate about efficiency measurement stems from an unusually large hysteresis in the typical current−voltage (*J*–*V*) measurement, in which the efficiency can depend on the history of the cell prior to the *J*–*V* measurement. Several authors have reported on this effect and speculated about the causes.[18−22] Some recent articles present cell designs that minimize this hysteresis.[23,24] In this article, we describe the hysteresis effect in additional detail. We examine the measurement of charge density and charge recombination times in MAPI cells with a particular aim to understand the *J*–*V* hysteresis and its roots in the material's chemistry.

The effect generally referred to as "hysteresis in the *J*–*V*" manifests itself in several ways. Most often, when a cyclic *J*–*V*

Received: January 22, 2015
Published: March 18, 2015

DOI: 10.1021/jacs.5b00761
J. Am. Chem. Soc. 2015, 137, 5087−5099

measurement is performed from 0 V to forward bias (to or beyond open circuit voltage, V_{oc}) and back, the return sweep shows a larger current, fill factor (FF), and V_{oc} than the forward sweep. This is illustrated in Figure 1a. The difference in efficiency between the two sweeps varies from a few percent, to as much as 90%, depending on the cell components, fabrication, and aging/degradation. It also depends on the sweep speed. Another manifestation of the hysteresis is as follows: The cell is placed at forward bias (e.g., 1.2 V) for a short time (e.g., 1 min). Then a $J-V$ is recorded, under light, from the forward bias potential back to 0 V. It is observed that the time at forward bias changes the state of the cell such that the subsequent $J-V$ shows a high current, FF, and V_{oc}. Unfortunately, in the majority of cases, the improvement is transient, requiring from seconds to minutes to decay when the cell is held at short circuit. From our observations, the most general description of the hysteresis effect is as follows: Assume the cell gives a particular steady state current under a given light intensity and voltage. When the cell is placed at any voltage further into forward bias, in light or dark, and is then returned to the original voltage, the photocurrent measured is higher than the previous steady state for some period of time.

In order to simplify further discussion of this characteristic of MAPI cells, we propose to give it a more specific name than "hysteresis", since hysteresis really only applies to a cyclic $J-V$ measurement. We wish to avoid words with existing physical meaning such as polling or polarizing until the actual physical mechanism is established. For lack of a better word, we refer herein to the "TEBB effect" from "temporary enhancement by bias". Holding a cell at a forward bias, prior to measurement at a lower bias, is thus "TEBBing" the cell. We find that the effect of previous TEBBing can be removed by holding the cell at reverse bias for a few seconds, thus we refer to this process as "de-TEBBing". Finally, if the cell is equilibrated at short circuit (SC) in the dark and then placed at some forward bias (e.g., maximum power point (MPP) or open circuit) in the light, the photocurrent (or V_{oc}) will increase with time as the cell internal state adjusts to the new applied potential. We call this effect "self-TEBBing". Self-TEBBing can take seconds, minutes, or even hours depending on the details of the cell.[18] Self-TEBBing can also occur under illumination at "short circuit" because the series resistance of the cell places the active layer under forward bias if photocurrent is flowing. The existence of the TEBB effect in MAPI cells has caused considerable confusion in the literature. As we show below, TEBBing affects more than just the $J-V$ efficiency. It is often not made clear whether the cell has or has not been purposely or accidentally TEBBed before any given measurement. Moreover, because some typical $J-V$ systems allow the cell to rest, illuminated, at V_{oc} before scanning the $J-V$ (independent of the $J-V$ direction), it is not always obvious to the authors of papers what degree of TEBBing may have taken place. Luckily the TEBB effect is becoming well-known, and the better articles are including specific details of preconditioning of the cells before the $J-V$ measurement.

Because of the high importance of the TEBB effect, other papers have examined some aspects of the effect. The original paper on the hysteresis suggested an origin in traps, mobile ions, or ferroelectric effects.[18] All three of these possibilities remain in the debate,[5,19,20,20,25] along with the addition of crystal size effects.[21] It has been proposed that an optimum mesoporous TiO_2 film thickness minimizes the $J-V$ hysteresis.[23] Alternatively, it has been suggested that cells with no TiO_2 layer can show zero hysteresis.[24] It has been suggested that nonstoichiometry, introduced in fabrication, can control the doping level in the MAPI films[16] and that passivation of surface nonstoichiometry can affect trap density.[17] In a recent conference, several authors highlighted the effects of excess methylammonium halide or excess lead halide on cell performance and hysteresis. However, there are usually multiple effects on the MAPI layer that result from a given change in precursor concentrations. Very recently, two additional papers have examined the hysteresis effect in MAPI cells. In one, the authors use variable scan rate $J-V$ measurements, voltage pretreatments, and voltage step experiments to examine mesoporous-TiO_2/MAPI cells similar to the ones examined here.[26] The authors conclude that ion movements in the MAPI during TEBBing are changing the built in potential. The second paper examines hysteresis in MAPI cells without mesoporous TiO_2 and also across horizontal MAPI layers between gold microelectrodes.[27] The authors provide electrical and visual evidence that ion drift is occurring during TEBBing. Although evidence is accumulating that ion drift is important, the existence of virtually hysteresis free cells using poly(3,4-ethylenedioxythiophene) (PEDOT) and phenyl-C_{61}-butyric acid methyl ester (PCBM) contacts complicates the picture.[24] If bulk ion drift is possible, it would also occur in these cells, yet no hysteresis is observed. Thus, electrode specific interactions seem to be required to generate the hysteresis effect.

In this paper, we examine the measurement of charge density and recombination in cells that exhibit significant hysteresis. Previous authors have used transient photovoltage (TPV), impedance, microwave absorption, and luminescence to examine recombination in MAPI cells.[5,9,10,28] However, as yet there is no consensus on the recombination lifetime or on the correct model for cell operation. In part, this may be because it has been assumed that when impedance is performed in the dark, the TEBBed or relaxed condition of the cell does not change with time and voltage. This is incorrect, as we will show below. How to characterize cells in the relaxed and TEBBed state is still not fully understood, not the least because of the short lifetime of these states in many cells. Here we look at cells with mesoporous TiO_2 layers under short and long periods of self-TEBBing at V_{oc}. We have chosen cells where the self-TEBBing time scale is ~100 s. In order to characterize cells at intermediate degrees of self-TEBBing, it is necessary to use techniques that require less than ~5 s to perform. Thus, we are led to measurements such as transient photovoltage (TPV), transient photocurrent (TPC), charge extraction (CE), and current interrupt (CI). Frequency domain measurements at applied voltage or V_{oc} can take too long to give a picture of the partially TEBBed or relaxed states, because the cell state will be evolving during the measurement. Our results highlight some important differences between MAPI cells and other related technologies such as dye-sensitized solar cells (DSSCs) and polymer/C_{60} cells. We also demonstrate that careful evaluation of the TPV lifetimes and charge densities is required and self-consistency checks are imperative when assigning kinetic features in new and complicated solar cell materials.

In this work, the device structure was FTO/sTiO_2/mpTiO_2/MAPI/SOT/Au, where FTO is fluorine-doped tin oxide, sTiO_2 indicates solid-TiO_2, mpTiO_2 is mesoporous TiO_2, and SOT is Spiro-OMeTAD. Most cells were made by the 1:3 ratio $PbCl_2$ and methylammonium iodide recipe. We will call this the MAPIC synthesis route; however, we refer to the product as

DOI: 10.1021/jacs.5b00761
J. Am. Chem. Soc. 2015, 137, 5087−5099

MAPI cells throughout, since there is debate whether any significant chloride remains in the cells. Any cells made with the iodide only recipe will be noted in text.

EXPERIMENTAL METHODS

The methylammonium lead iodide (MAPI) solar cells were fabricated using modifications of standard recipes.[29] Methylammonium iodide (MAI) was prepared as previously described.[30] Fluorine-doped tin oxide (FTO) coated glass (TEC 15, Hartford Glass Co.Inc.) was patterned by etching with zinc powder in 2 M HCl, cleaned with DI-H_2O and isopropanol and heated at 450 °C for 30 min. A dense TiO_2 (~100 nm) blocking layer ($sTiO_2$) was deposited on the FTO glass substrates via spray pyrolysis.[31] An ~400 nm layer of mesoporous titanium dioxide, $mpTiO_2$ (Dyesol DS-18NRT or G24i (22-TB)), was applied by spin coating onto the FTO/$sTiO_2$ substrates, followed by sintering at 450 °C for 30 min. For the "chloride route", the deposition solution was prepared by mixing $PbCl_2$ (Sigma-Aldrich) with MAI (1:3 molar ratio) in DMF. The solution was filtered through 0.2 μm syringe filters (PTFE). This solution was transferred into the glovebox for all subsequent steps. The solution was placed onto the $mpTiO_2$, allowed to sit for 45 s, and then spun at 2000 rpm (2000 rpm/s ramp) for 60 s. The coated substrates were dried at room temperature for 30 min and then at 100 °C for 90 min, resulting in a MAPI layer with an ~300 nm capping layer over the $mpTiO_2$. The deposition solution of SOT was made as follows: 93 mg of SOT was dissolved in 1 mL of cholorbenzene; 175 mg lithium bis-trifluoromethanesulfonimide (LiTFSI) was dissolved in 1mL of acetonitrile; 32 μL of the LiTFSI solution was added to the SOT solution along with 10 μL of *tert*-butyl pyridine. The SOT solution was placed on the MAPI layer and then spun at 2000 rpm (2000 rpm/s ramp) for 60 s. This process resulted in an ~300 nm film of SOT. A gold counter electrode of ~80 nm was evaporated onto the SOT layer. Cell areas measured were 0.08−0.2 cm^2. The devices were encapsulated in a nitrogen-filled glovebox immediately after electrode evaporation using a glass coverslip and a Surlyn (DuPont) gasket. The seal was made by heating the gasket around the cell with the tip of a soldering iron.

Calibrated current/voltage (J−V) measurements were performed under simulated 1 sun illumination (AM 1.5) using a 150 W xenon lamp with an AM 1.5 global filter. Calibration was performed with a silicon photodiode before measurements. The J−V measurements were typically performed as follows. First, the cell was at open circuit (OC) at ~1 sun for a few minutes while it was aligned in the simulator and while other cells on the same plate were run. For the measurements, the short circuit current (J_{sc}) was first allowed to stabilize (20−100 s), and then the cyclic J−V was swept toward forward bias and return at ~0.1 V/s. The data were recorded using a Keithley 2400 sourcemeter. Other J−V measurements were performed under 1 "sun equivalent" light from white light-emitting diodes (LEDs) using various voltage and light sequences as specified in the text.

Transient and charge extraction measurements were performed using the IC designed and built TRACER system.[32] The TRACER system provides bias light from 10 1 W white LEDs with focusing optics (Lumileds). Pulse illumination is provided with 5 1 W red LEDs. Both bias and pulse are controlled by fast solid-state switches. Fall time of the pulse is ~300 ns. Pulse times were 10 μs unless otherwise stated. Data were collected on a 16 bit data acquisition board with 0.8 μs/point resolution. Averaging was employed to achieve a noise level below 50 μV to allow detection of both fast and slow components of the decay. As well as transients, current and voltage can be measured while bias light, voltage, and SC/OC status are varied in in an arbitrary sequence for up to 100 different steps. The steps are accomplished with three fast solid-state switches with <1 μs switching and synchronicity. Charge density at V_{oc} was measured by charge extraction by integrating the current pulse after the cell had been rapidly switched from open circuit under light to short circuit in the dark. Capacitance was measured using transient photovoltage and transient photocurrent results as published previously.[33,34] A slightly modified procedure was used, as explained along with the results.

Current interrupt (CI) measurements were also made as a function of J_{sc} at different bias light levels. Current interrupt voltage is measured by first allowing the cell to equilibrate at short circuit under illumination. At time zero, the light is switched off and the cell is simultaneously switched to open circuit. The V_{oc} transient that follows is measured. The voltage transient is explained as follows. When the cell is illuminated at SC, the balance of charge generation and transport creates a steady state concentration of excess electrons and holes. These excess holes and electrons create a separation of the electron and hole quasi-Fermi levels in the interior of the photoactive layer. The object of the CI measurement is to determine this separation or at least changes in it. If the cell at short circuit is quickly switched to open circuit and the light is simultaneously shut off, the existing field across the cell (or concentration gradients) will continue to move the charges toward the electrodes. This will cause a buildup of voltage on the external contacts. The voltage will grow until the charge distribution reaches equilibrium. The voltage will then start to decline as the charges recombine. If the transport is sufficiently faster than recombination, the peak CI voltage will be related to the separation of the quasi-Fermi levels in the interior of the cell at SC. The charge concentration at a given J_{sc} is related to the charge mobilities. For a heterojunction cell, the quasi-Fermi level separation is related to the charge concentration, the band offsets, and the band density of states. A shift in the peak CI voltage caused by some treatment is thus most likely a change in band offsets or possibly a change in the charge mobilities. For completeness, we note that changes in CI voltage might also result from changes in an unbalanced distribution of hole and electron traps in the photoactive layer.

RESULTS

Because several different subjects are covered in the results section, we provide a short summary of the logical flow here. In Figure 1 and related text, we present the basic characteristics of the hysteresis effect as it appears in the J−V curves and in a new experiment based on simultaneous changes in applied voltage and light intensity. In the remaining figures, we characterize some different physical aspects of $mpTiO_2$/MAPI cells and examine how the results illuminate (or do not) the hysteresis effect. In Figure 2, we provide a measure of the excess charge density in the cell at open circuit (OC). We find that there are two different kinds of stored charge, and we posit that one is made up of electrons and holes and the other of ions and/or dipoles. In Figure 3 and text, we provide an independent measurement of charge density at OC. We argue that this second technique allows us to quantify only the electronic charge. The electronic charge data indicate that the hysteresis effect is linked to a band edge offset change that occurs when the cell is held at forward bias. In Figure 4 we present the current interrupt voltage (CIV) as a function of light intensity at short circuit. Evidence for a band edge shift also shows up in the CIV, supporting the interpretation of Figure 3. Figure 5 and Table 1 and the discussion thereof serve two purposes. The first is to establish the correct time scale for electron/hole recombination in TiO_2/MAPI cells, which has been under debate. The second is to provide support for our assertion that the charge measurements in Figure 3 are electronic charge. If that assertion seems a priori reasonable to the reader, the section can be skipped. We also observe (Figure 5) that the small perturbation photovoltage decays are all double exponential. We propose that both the time constants relate to electron/hole recombination. In order to convince ourselves, and the reader, that this is possible, in Figure 6 and text, we present two reasonable electronic models that create double exponential decays similar to those measured. The last two sections discuss and discard some alternate explanations for the

DOI: 10.1021/jacs.5b00761
J. Am. Chem. Soc. 2015, 137, 5087−5099

data in Figure 5 and estimate the impact of uncertainty and error on the conclusions from Figure 3.

Regarding the usage of "1 sun", all measurements except for those in Figure 1a use white LEDs for bias light. There is a large spectral mismatch using white LEDs to illuminate MAPI cells, thus it is not technically correct to refer to any intensity of the LED bias light as "1 sun". A given LED light intensity was defined as "1 sun equivalent" if it gave approximately the same J_{sc} as the cell under the solar simulator. In the case of the data herein, the "1 sun equivalent" intensity was slightly too high, giving 10−20% higher maximum photocurrent compared with the solar simulator. In general, this offset has no impact on the conclusions, since all measurements used the same bias light and no energy efficiency calculations are made. For simplicity, we retain the use of "1 sun" despite the offset. Where absolute values are important, the offset will be noted.

***J*−*V* Measurements, Chronoamperometry, and Hysteresis.** Figure 1a shows the cyclic *J*−*V*s of a typical mpTiO_2/MAPI/SOT cell made at ICL. The initial *J*−*V* (green) gave an efficiency of 8.2% on the forward sweep and 9.6% on the reverse sweep, thus a hysteresis of ∼20%. The dashed line in Figure 1a is a fast reverse sweep *J*−*V* after holding for 60 s at 0.9 V forward bias (TEBBing). The "V_{oc}" in the TEBBed condition was 0.89 V, and the "efficiency" was 12.6% (see Introduction for our use of the verb "TEBBed"). After a month of storage in room lights with occasional 1 sun exposure, the stable J_{sc} began to decline and the hysteresis to increase (Figure 1a). After 4 months of storage, the *J*−*V* efficiency was down to 2.5% and 6.2% for the forward and reverse scan (Figure 1a, red line). The steady state efficiency at the MPP declined to ∼2.5% as well. We note that even after 4 months, a *J*−*V* similar to the dashed line in Figure 1a could still be achieved by TEBBing the cell for ≥60 s at 1 V forward bias and performing a very fast reverse scan (2 V/s). This kind of *J*−*V* could be used to give a false impression of stability, when in fact the steady state efficiency had decreased dramatically. Figure 1b shows the importance of pretreatment on the *J*−*V* measurement of the same cell, aged 100 days. In Figure 1b, the cell was allowed to relax for 25 min in the dark before the first *J*−*V* measurement with the shortest TEBBing time. Between each successive *J*−*V* measurement, the cell was deTEBBed for 1 min at −1 V, relaxed for 2 min at 0 V, and TEBBed for the indicated time at 1 V, and then the light was turned on and the voltage was scanned at −2 V/s. It is apparent that the pretreatment has a huge effect on this cell, once it has been fully relaxed in the dark. The "efficiency" measured from these *J*−*V* measurements would vary between 0.1% and 9%. This behavior is not restricted to aged cells. If a fresh cell shows significant hysteresis, it gives similar results. Also, it is clear that sufficient reverse bias is able to overcome the lack of TEBBing. At −4 V, the cell shows ≥22 mA/cm^2 photocurrent without any TEBBing (Figure S1, Supporting Information). Thus, it would seem that the low efficiency without TEBBing is due to poor collection rather than poor charge generation.

A deeper view of the TEBBing effect can be found by examining the photocurrent and dark current at a fixed forward bias (Figure 1c). The black line in Figure 1c is the current that flows after a jump from 0 to 0.9 V forward bias in the dark. We assume that the dark current flows as hole/electron recombination in the bulk of the MAPI layer or at one of the MAPI interfaces. Under this assumption, the increase in dark current with time is due to better charge injection into MAPI or better charge transport within the MAPI layer. We believe a

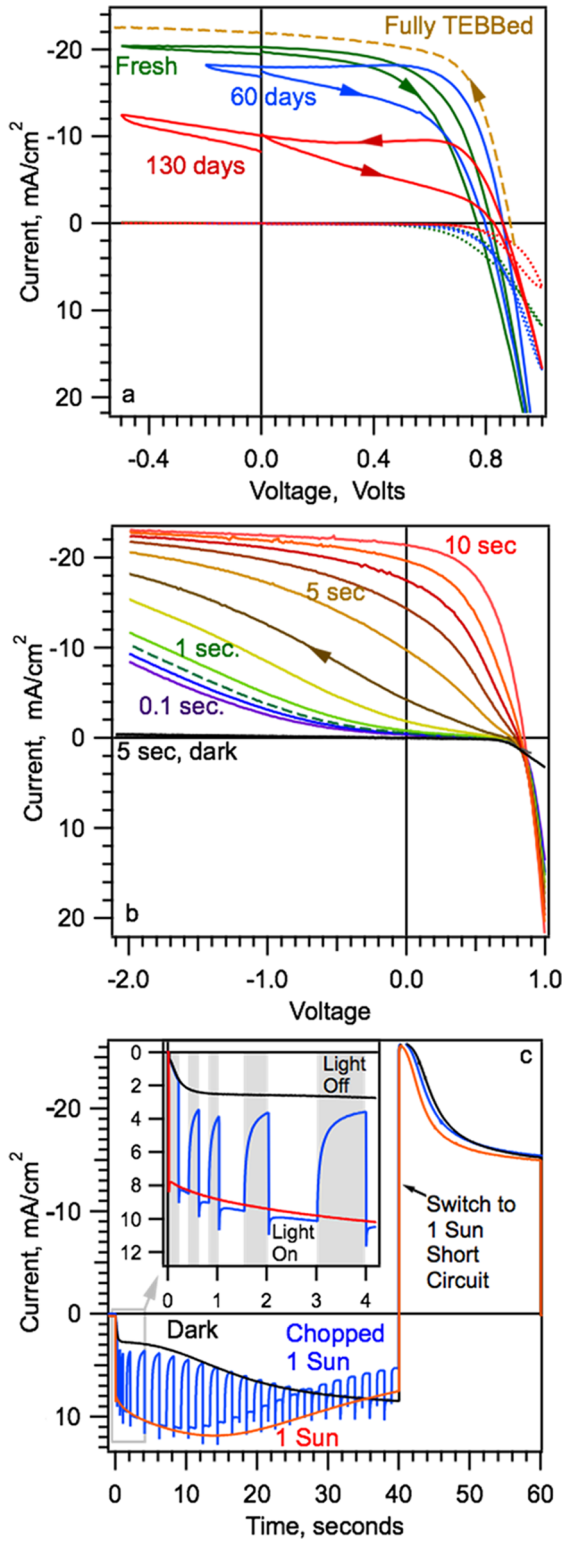

Figure 1. (a) *J*−*V*s for a typical mpTiO_2/MAPI/SOT cell vs aging of the cell. Light source: 1 sun AM1.5 simulator. The cell was fabricated and sealed in a glovebox. (b) Reverse direction *J*−*V*s of the same cell after TEBBing at 1 V forward bias with TEBBing time as labeled. (c) Forward bias current of the same cell at 0.9 V in dark (black), light (red), and chopped light (blue). At 40 seconds, the cell is placed at short circuit and the light is turned on. Inset: magnification of the first 4 s of forward bias. For the chopped light curve (blue), the gray areas represent time in the dark. Light source for parts b and c was ∼1 sun equivalent white LEDs. Cell age 100 and 60 days for parts b and c, respectively.

DOI: 10.1021/jacs.5b00761
J. Am. Chem. Soc. 2015, 137, 5087−5099

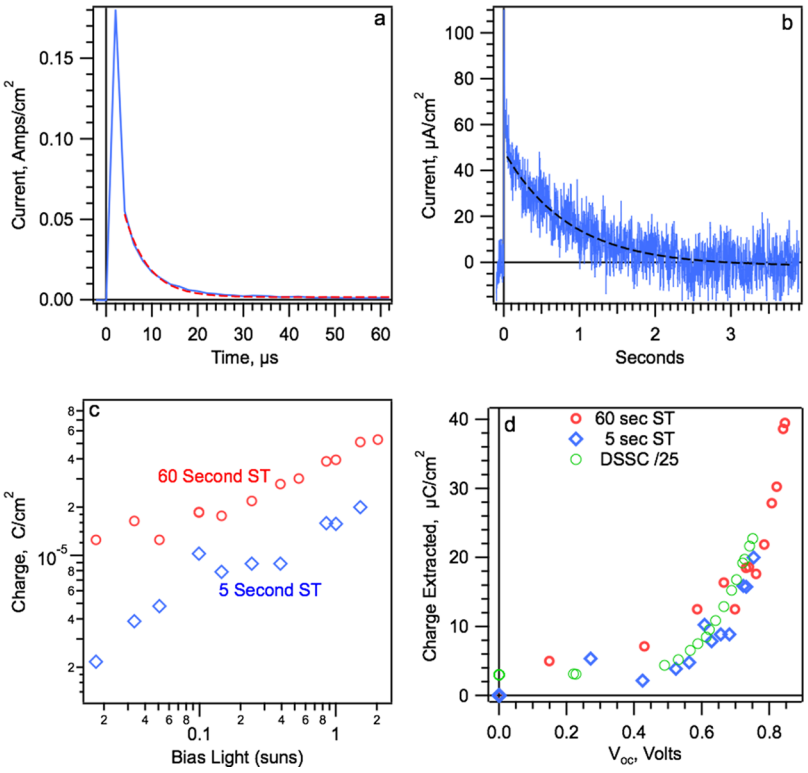

Figure 2. (a) Charge extraction current after 60 s self-TEBBing at 1 sun, V_{oc} = 0.88 V. Red dashed line is an exponential fit. (b) The same charge extraction transient viewed at a longer time scale. Black dashed line is a different exponential. (c) Charge extracted from V_{oc} vs bias light applied, for long and short self-TEBBing (ST) times. (d) Charge extracted from V_{oc} vs V_{oc} for long and short self-TEBBing times. Green circles are charge extraction data from a typical DSSC with a 7 μm mpTiO_2 film, normalized down by a factor of 25.

decreased injection barrier at one of the MAPI contacts is most consistent with other data shown below. Along the black line, at 40 s, the cell is switched to SC and the 1 sun light is turned on. A large photocurrent, 26 mA/cm^2, is recorded that decays to a steady state value over 20 s. (The maximum J_{sc} in Figure 1c is about 20% higher than that in Figure 1a because the LED bias light intensity was equivalent to about 1.2 "suns", as explained above.) The transient photocurrent in Figure 1c is not a capacitive discharge. The capacitive discharge caused by switching from 0.9 V to SC in the dark decays to <1 mA/cm^2 in <100 μs (Figure S1b, Supporting Information). The transient photocurrent results from a semistable TEBBed state of the cell. As noted by others, the TEBBed state has a near 100% photon to current conversion efficiency at SC. We note that 2 s of de-TEBBing at −1 V removes most of the effect of 40 s TEBBing at forward bias. The red line in Figure 1c is the current that flows at 0.9 V forward bias under 1 sun illumination. Initially, the forward bias current is ∼3 times larger in the light, a feature often referred to as a photoshunt. (We use photoshunt herein without indicating it can be viewed as a parallel resistance.) After ∼15 s, the photoshunt begins to decrease, and at 35 s the current under light crosses the dark current curve, and a "photocurrent" is recorded. At 40 s, the cell is set to SC, still under 1 sun illumination. At SC a photocurrent peak is recorded that is identical to that shown after 40 s TEBBing in the dark. The blue line in Figure 1c is the current recorded at 0.9 V forward bias when the 1 sun light is chopped with varying intervals. The inset shows a magnification of the first 5 s. When the light is turned on, for example, at 0.2 s, there is an immediate jump from the dark curve to the light curve. This jump takes ≲3 ms; thus we believe that the photoshunt must be electronic in nature as opposed to moving ions or dipoles. However, after the light is turned off (e.g., at 3 s), the photoshunt decays much more slowly, requiring about 1 s to disappear. The photoshunt is almost certainly not an electronic photoconductivity effect in the MAPI layer, where charges have lifetimes of hundreds of nanoseconds.[8,35,36] After ∼10 s in chopped light, the net photoshunt begins to decrease, and after 24 s the light on periods show positive photocurrent instead. At 40 s, the cell is short circuited with the light on, again giving 26 mA/cm^2 and a similar decay.

The first important observation regarding Figure 1c is that the hysteresis in MAPI cells is not a light driven process. The photocurrents (and the J−V measurements, not shown) that result from TEBBing at forward bias in the light or dark are almost identical. We observe this to be true over many cells including those with mpTiO_2, planar cells, cells made with the MAPIC or iodide only procedures, and even cells with formamadinium instead of methyl ammoniun. A few authors have asserted that hysteresis is a light driven effect.[10,18] Instead, we note that the faster rise of the photocurrent under chopped light (Figure 1c, 10−30 s), relative to the fully illuminated case, indicates that light actually interferes with the beneficial effects of TEBBing to some extent. A second conclusion is that effects of TEBBing do not arise from a single physical process. As the photocurrent increases after 25 s, there is still a negative transient immediately after the light is turned off (see the light off transient at 38 s). This indicates that the photocurrent measured is a balance between charge generation and photoshunting. We believe the photoshunting is not related to the positive influence of TEBBing, thus there are at least two separate processes evolving in Figure 1c. The evolution of the

DOI: 10.1021/jacs.5b00761
J. Am. Chem. Soc. 2015, 137, 5087−5099

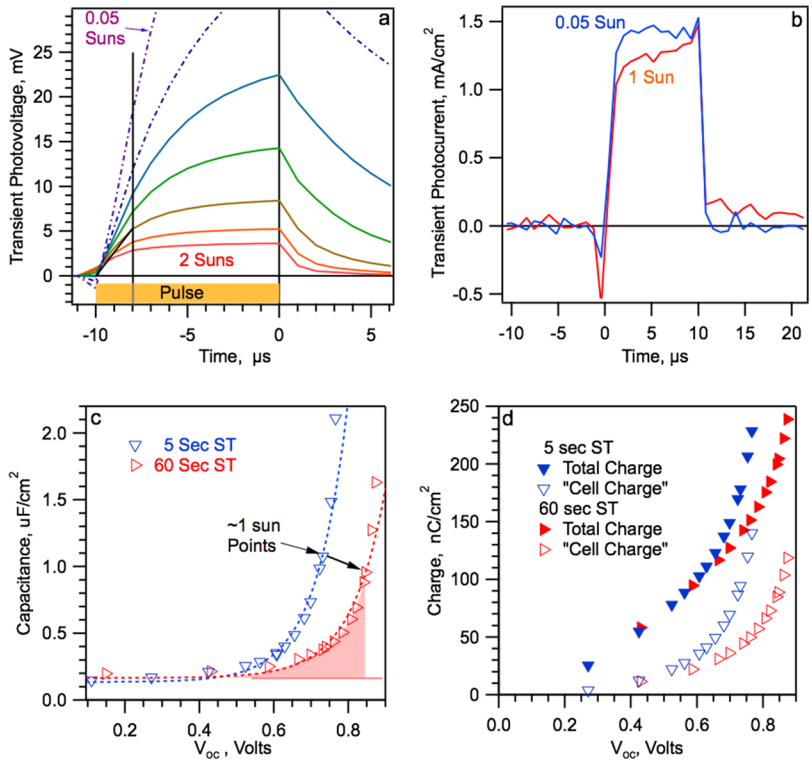

Figure 3. (a) Transient photovoltage (TPV), after 60 s self-TEBBing (ST), using a 10 μs red pulse on top of a white bias light, the latter varying from 0.05 sun to 1 sun. Data is from the same cell shown in Figures 1 and 2. Cell age 30 days. *Y*-axis is scaled to show rise rate; complete transients are shown in Figure S3e, Supporting Information. (b) Transient photocurrent (TPC) data taken at short circuit using the same pulse, with white bias light as indicated. (c) Capacitance vs V_{oc} for the cell after 5 and 60 s self-TEBBing at each V_{oc}. Capacitance derived from TPV and TPC as explained in the text. (d) Integrated capacitance vs V_{oc}. "Cell charge" refers to the integral of the capacitance above the flat baseline observed at low voltage. The "cell charge" of the 60 s self-TEBBed cell at 1 sun is indicated by the shaded red area in panel c.

dark current (fast increase for 0.3 s, plateau, then further increase) hints at three separate processes.

Charge Density from Charge Extraction. Critical to understanding the physics of MAPI cells is measurement of the charge density under various conditions. In DSSCs and polymer cells, the charge extraction (CE) measurement has been found to be accurate and useful (see Experimental Methods for details).[33,37,38] Figure 2a shows the charge extraction current collected after the cell was switched from 1 sun OC to dark SC. The peak current measured was 180 mA/cm^2. The current decays to <1 mA/cm^2 in about 50 μs. Most of this decay is nicely fit by an exponential with a lifetime of ~6 μs. When the charge extraction current is integrated out to 50 μs, the charge collected is ~8 × 10^{-7} C/cm^2. With a 500 nm cell thickness, this would correspond to an average charge density of 1 × 10^{17}/cm^2, if the charge were uniformly distributed (which seems unlikely). Although the charge extraction current decay in Figure 2a looks complete at 50 μs, closer inspection shows that it is not (Figure 2b). There is a second portion of the decay with a maximum current of 50 μA/cm^2 that decays exponentially with a lifetime close to 1 s. Although the current is 1000 times lower than that of the fast component, the time is sufficiently long that the integrated charge collected is about 50 times higher, ~3.6 × 10^{-5} C/cm^2. The two very disparate time scales give some clue that there are least two ways in which photogenerated charge is stored in this system. Figure 2c shows the total extracted charge from V_{oc}, using 4 s integration, as a function of light intensity. In Figure 2c, the blue diamonds show the amount of charge extracted after 5 s 1 sun light exposure at OC (i.e., "self-TEBBing"). The red circles show the amount of charge extracted after 60 s of self-TEBBing at the 1 sun V_{oc} (Figure S2a, Supporting Information, shows the evolution of the V_{oc} under self-TEBBing at 1 sun and 1/10 sun). It is apparent in Figure 2c that longer self-TEBBing increases the amount of extracted charge by a factor of 2.5 for a given light level. Figure 2d shows the same charge data plotted versus V_{oc}, along with normalized data from a dye sensitized cell. In contrast to Figure 2c, at a given V_{oc} the extracted charge is similar for the long and short self-TEBBing. There is some hint of larger charge for a given V_{oc} after longer self-TEBBing, but we have not found a convincing trend over several measurements and cells. Figure 2d also shows the charge extraction results for a typical DSSC, divided by 25 to account for the difference in the mpTiO_2 thickness. The charge vs V_{oc} trend is remarkably similar for the two types of cells. The charge stored in a DSSC is known to be mixed ionic/electric charge, where electrons in TiO_2 are charge balanced by ions in solution inside the mesoporous TiO_2 network. One might speculate that the charge in the MAPI cell is also electrons in TiO_2 and mobile ions in MAPI. However, we caution there are important differences in the time evolution of the charge extraction current. In DSSCs, 95% of the extracted charge is collected in the first 40 ms, leaving a current of <1 μA/cm^2 after 0.1 s (Figure S2b, Supporting Information). In the MAPI cell, it takes over 2 s for 95% of the charge to be collected. If there are moving ions in the MAPI/SOT, they are moving much slower than those in the electrolyte of a DSSC. There are additional problems with assigning the charge extraction results to "electrons in TiO_2", as we detail below.

DOI: 10.1021/jacs.5b00761
J. Am. Chem. Soc. 2015, 137, 5087−5099

Charge Density from Differential Capacitance. "Differential charging" is another technique that has been used to measure capacitance and thus charge density in both DSSCs and polymer/PCBM solar cells. It was found in both these cell types that the differential charging method gives essentially the same stored charge as the charge extraction method.[33,34,38] We show herein that this is not true for mpTiO$_2$/MAPI cells. The differential capacitance can be measured by combining transient photovoltage (TPV) and transient photocurrent (TPC) results to find $C = dQ/dt/(dV/dt)$. Figure 3a shows representative TPV transients taken using a 10 μs square pulse (650 nm) at different bias light intensities. In the early part of the pulse, the increase in charge separation flux causes an increase in charge density that is approximately linear in time. For small perturbations, this gives rise to a linear increase in the voltage, which is dV/dt. Figure S3a, Supporting Information, compares TPV transients for 5 and 60 s self-TEBBing. In order to find dQ/dt during the pulse, we use the photocurrent transients. Figure 3b shows photocurrent transients at SC made using the same LED pulse, with bias light intensities of 1 sun and 0.05 suns. The plateau transient photocurrent at SC can be used as an estimate of the charge generation flux using the same pulse at OC. The estimate is reasonable under the following assumptions: (i) that their are no significant collection losses at short circuit and (ii) that charge generation efficiency is similar at short circuit and open circuit. Either of these assumptions could be wrong. However, for the measurements presented here, we can show (below) that any corrections required would not change the main conclusions drawn from the data. We note that a better way to find dQ/dt during TPV is to measure the transient absorption (TA) of the charges simultaneously with the TPV.[39] The TA can then be converted to charge if the absorption coefficient is known. These data are not available yet for the MAPI system.

Figure 3c shows the differential capacitance at V_{oc} for a range of light levels from 0.005 to 2 suns (Figure S3b, Supporting Information, shows similar data for additional cells). Integration of the capacitance vs voltage gives the charge stored (Figure 3d). In Figure 3d, the solid symbols are the integral of the full capacitance and the open symbols are the integral of the part of the capacitance above the flat baseline between 0 and 0.3 V. Assuming that the flat baseline represents the charge on the contact electrodes, the open symbols represent the charge stored in the bulk of the solar cell, including at the internal interfaces.

There are two notable features of Figure 3c,d. The first is the magnitude of the capacitive charge relative to the charge measured by charge extraction. The total capacitive charge stored at 1 sun is ~0.2 μC/cm^2. This is 200 times smaller than the 40 μC/cm^2 measured in the charge extraction experiment (Figure 2d). Thus, unlike in DSSCs and polymer cells, differential capacitance and charge extraction give very different results in MAPI cells. Interestingly, the capacitance in Figure 3c is also about 10 times less than would be expected for a solid-state dye-sensitized cell using a similar mpTiO$_2$ film thickness.[40−42] This implies either that the traps in the TiO$_2$ are passivated by the MAPI or they are not all accessible at a given potential. The latter is a reasonable result for a p-i-n structure where the potential drops across the MAPI and mpTiO$_2$/MAPI layers. At any $V_{oc} < V_{bi}$ (where V_{bi} is the built in potential), the Fermi level will be farther below the TiO$_2$ conduction band edge for positions farther from the FTO contact. Thus, only the TiO$_2$ electron states near the FTO will be filled to the level implied by the V_{oc}.

The second notable feature in Figure 3c is the ~120 mV right shift of the capacitance vs voltage curves when the self-TEBBing time is increased from 5 to 60 s. We have also observed this shift for mpTiO$_2$/MAPI cells made using other TiO$_2$ sources and somewhat different MAPI deposition procedures (Figure S3b, Supporting Information). In DSSCs, shifts of the capacitance vs voltage are frequently observed between cells and within cells with time. These shifts occur when the acid/base characteristics of the electrolyte are changed intentionally or change with time or light exposure.[43,44] In DSSCs, the shift in the capacitance curves has been assigned to adsorption/desorption of ions or dipoles that change the electric field between the TiO$_2$ and the electrolyte. For this reason, it is tempting to assign the shifts observed for mpTiO$_2$/MAPI cells to ion movements or dipoles near the surface rather than to, for example, bulk ferroelectric effects. The shift may be related to the aligned dipoles found in some modeling of the TiO$_2$/MAPI interface.[45] More certain assignment must await further evidence.

Current Interrupt Voltage and Band Offsets. Current interrupt voltage is another way to examine shifts in internal electric fields between treatments and samples.[34] The method measures the voltage that can be generated at OC by the charge that is accumulated at SC (see Experimental Methods section for details). Figure 4a compares the current interrupt voltage transient from two similar J_{sc} values, for 5 and 60 s self-TEBBing at SC. In each case, there is a voltage rise as charge is

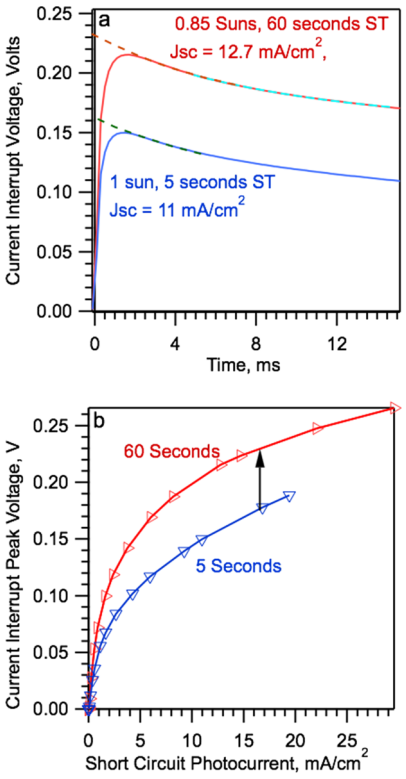

Figure 4. (a) Voltage transients following current interrupt from 1 sun short circuit for 5 and 60 s self-TEBBing (ST) at J_{sc}. Bias light level chosen to give similar photocurrents, as indicated. Same cell as previous figures. (b) Current interrupt voltage peak vs J_{sc} for 5 and 60 s self-TEBBing times.

DOI: 10.1021/jacs.5b00761
J. Am. Chem. Soc. 2015, 137, 5087−5099

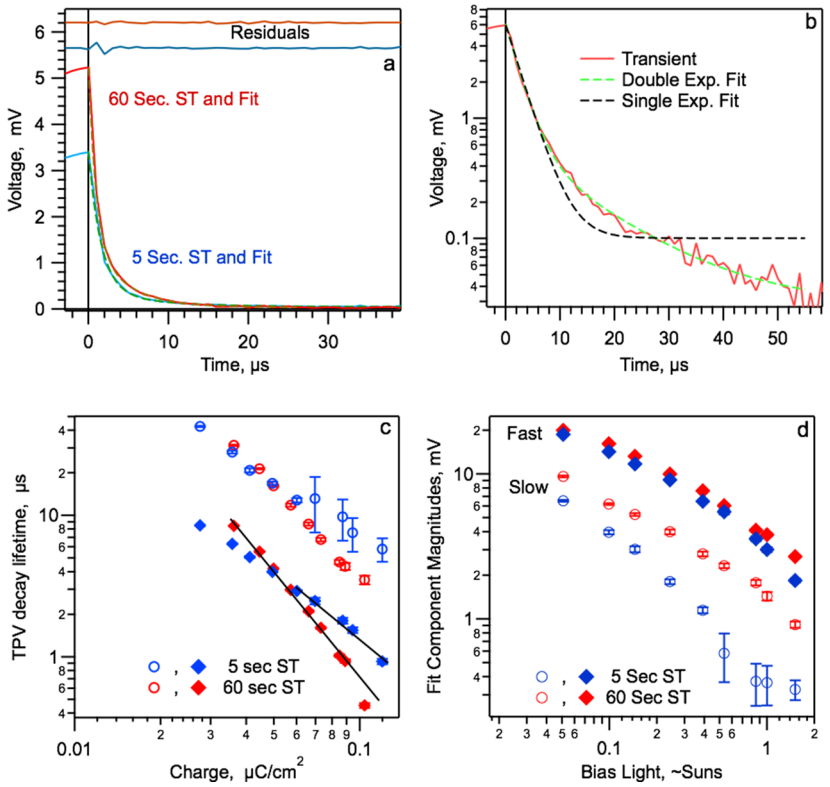

Figure 5. (a) TPV decay at 1 sun after 5 and 60 s self-TEBBing (ST) with double exponential fits and residuals. (b) Log scale presentation of the same data showing the need for a double exponential fit. (c) Shorter and longer lifetimes from the double exponential fits vs the cell charge. The charge is the integrated capacitance above baseline ("cell charge") from Figure 3c. (d) Magnitudes of the short and long decay components vs bias light.

transported toward the contact electrodes, followed by a decay as the charge recombines. Figure 4b shows the peak CI voltage recorded (at ~2 ms) for a series of different bias light levels and for 5 and 60 s self-TEBBing at SC. In Figure 4b, longer self-TEBBing time gives an ~60 mV higher CI voltage for a given photocurrent. (It is also possible to find the initial CI voltage by extrapolation of the voltage decay back to time zero (dashed lines in Figure 4a). The extrapolation does not change the shift between the 5 and 60 s self-TEBBed conditions.) The peak CI voltage for a given current is determined by the amount of charge required to carry that current and how much voltage that amount of charge generates after the cell is switched to OC. If the mobilities of the charges remain similar, so that the amount of charge remains the same, an increase in CI voltage indicates an increase in the band offset at the voltage generating interface(s) in the cell. It has been suggested that the V_{oc} in the cell is primarily generated by the electron extraction layer/MAPI contact.[12] If so, then the shift in the CI peak voltage in Figure 4b indicates changes in dipole/charge density at the $mpTiO_2$/MAPI and/or $sTiO_2$/MAPI interfaces. The capacitance in Figure 3c, 2 $\mu F/cm^2$, is similar to the capacitance measured for planar TiO_2 films facing electrolyte. On the other hand, we have performed some initial measurements of capacitance for MAPI cells with different $mpTiO_2$ thickness. There appears to be a trend for larger capacitance with thicker $mpTiO_2$, but we would not say the case is closed (Figure S3d, Supporting Information). It has also been suggested that the V_{oc} in MAPI cells is developed across the MAPI layer.[11] This could also be consistent with the low capacitance in Figure 3b, although the hypothesis may require a chemical potential gradient in the MAPI that has not yet been detected. We note last that an alternative explanation for the 60 mV shift in CI voltage in Figure 4b would be an ~3 fold *decrease* in charge mobility after 60 s self-TEBBing. This would cause an ~3 fold increase in the charge for a given J_{sc}, consistent with Figure 4b. A significant decrease in charge mobility in the longer self-TEBBed condition does not seem likely, given that self-TEBBing increases the photocurrent.

Recombination Lifetime. We now turn to the decay dynamics of the photovoltage transients and their possible interpretation as recombination time constants. Figure 5a shows the TPV decay under 1 sun bias light after 5 and 60 s self-TEBBing. Both of these decays are strongly double exponential. Figure 5a shows the double exponential fits and the residuals. In both cases, the fast part has a lifetime of 1−2 μs and the slow part 5−10 μs. Figure 5b highlights the double exponential nature of the decay and the poor quality of a single exponential fit. This is in agreement with several previous reports of TPV decays on MAPI cells.[8,15] Figure 5c shows the two TPV lifetimes for both the short and long self-TEBBing times, as a function of cell charge. The fast and slow lifetimes differ by a factor of ~5. The error bars (shown as 2 standard deviations) are usually <5% and are <20% for all cases. The fast and slow lifetimes are thus significantly different at >90% confidence level for all transients. The double exponential nature of the decays has also been verified using 20 ns laser pulses as excitation and a data time resolution of 8 ns (Figure S5a, Supporting Information).

Surprisingly, self-TEBBing causes less than a factor of 2 change in either the long or short TPV lifetimes (Figure 5c). Moreover, at one sun, both the short and long lifetimes get shorter with increasing self-TEBBing time. This is despite the

DOI: 10.1021/jacs.5b00761
J. Am. Chem. Soc. 2015, 137, 5087−5099

Table 1. Charge in Device, Transient Photovoltage (TPV) Lifetime, and Calculated Recombination Current (J_{rec}) at V_{oc} for Long and Short Self-TEBBing Times at V_{oc} under Two Different Bias Light Intensities[a]

TEBBing time (s)	bias light (~suns)	charge meas. type[b]	charge (nC/cm^2)	component of TPV decay time	TPV decay lifetime[c] (μs)	order factor	J_{rec}, (mA/cm^2)	line no.
60	1	C	89	**short**	**0.93**	**4.4**	**22**	**1**
				long	*4.4*	*2.9*	*6.9*	*2*
60	1	T	210	short	0.93	5.8	39	3
				long	*4.4*	*4.4*	*11*	*4*
60	0.1	C	44	**short**	**5.5**	**3.1**	**2.6**	**5**
				long	*21*	*3*	*0.7*	*6*
60	0.1	T	140	short	5.5	5.1	5	7
				long	*21*	*4.6*	*1.4*	*8*
5	1	C	94	**short**	**1.5**	**2.7**	**23**	**1a**
				long	*7.5*	*2.2*	*5.6*	*2a*
5	1	T	180	short	1.5	4.3	28	3a
				long	*7.5*	*3*	*8*	*4a*
5	0.1	C	36	**short**	**6.3**	**2.4**	**2.4**	**5a**
				long	*28*	*2.8*	*0.46*	*6a*
5	0.1	T	103	short	6.3	3.3	4.9	7a
				long	*28*	*4*	*0.9*	*8a*
60	1	CE	40000	short	0.93	3.1	14000	9
				long	*4.4*	*2.7*	*3000*	10

[a]J_{rec} values highlighted in the **bold** lines are physically reasonable (as described in the text). [b]The charge in the device was determined either by integrating the differential capacitance measurements up to V_{oc} (total charge, T) or integrating the capacitance above the baseline value ("cell charge", C) up to V_{oc}. Alternatively the charge was determined from charge extraction measurements (CE); see text and Figure 3d for full details. [c]The TPV lifetimes were well fit with double exponential functions; the calculations of J_{rec} were performed using either the **short** or *long* component of these decays.

fact that self-TEBBing increases the V_{oc} by 0.12 V. Plotting the TPV lifetime vs bias light gives the same picture (Figure S5c, Supporting Information). Figure 5d shows the magnitude of the long and short lifetime component of the decay for 5 and 60 s self-TEBBing time. We see here that the main effect of self-TEBBing on TPV is to increase the absolute and relative magnitude of the slow part of the TPV decay. For example, at 1 sun, self-TEBBing increased the transient height from 3.4 to 5.2 mV, and the slow component increased from 10% to 27% of the signal. Although these trends are interesting, overall, the TPV results indicate that decreased recombination rate is *not* the cause of the large increase in V_{oc} seen during the self-TEBBing of the cell. This result supports the aforementioned hypothesis that the increase in voltage is due to changes in band offset, most likely from changes in interface surface charge caused by moving dipoles or ions.

Our data show that at 1 sun, >70% of the transient photovoltage decays with a lifetime of ~1 μs. This result falls at the short end of what has been reported in the literature. Bisquert et al. recently reported 1 sun TPV lifetimes that varied from 100 to 2 μs, depending on the material (MAPI or formamadinium lead iodide) and the fabrication procedure (single or two step).[5] They came to the conclusion that these decay times could not be associated with electron/hole recombination. Most other papers using transients or impedance have found a 90−200 μs characteristic time, which they have assigned to charge recombination. Unfortunately only one of the TPV based papers presented raw transient data. In that paper, the photovoltage transient had a 20 μs rise time that would have obscured any fast decay components that might have been present.[8] We have also found that the shape of the transient decay depends on the length of the pulse used to create the transient. For example, square pulses ≥20 μs in length generate decays with a third component that has a lifetime in the 200 μs to 1 ms range (Figure S5d−f, Supporting Information). The magnitude of the third decay component grows with pulse length. To avoid the third component, we have used a pulse length of 10 μs for the data presented here.

Implied Recombination Flux at V_{oc}. In a new technology such as perovskites cells, it is risky to assume, without verification, that a given impedance signal or photovoltage decay lifetime corresponds to a particular process. We propose here that the 1 μs lifetime that we observe in TPV is a result of the predominant electron/hole recombination channel, and thus the average charge lifetime, at the 1 sun V_{oc}, is close to 1 μs in these cells. In the paragraphs below, we test this assignment for consistency with the photocurrent and charge density. We do so by combining the TPV lifetimes in Figure 4c with the charge in Figure 3d to find the implied "recombination current" inside the cell. The recombination current (J_{rec}, with units mA/cm^2) is calculated with eq 1.

$$J_{rec} = Q(V_{oc})/(\tau(V_{oc}) \times OF) \quad (1)$$

DOI: 10.1021/jacs.5b00761
J. Am. Chem. Soc. 2015, 137, 5087−5099

where Q is the charge in the cell, τ is the TPV lifetime, and OF is the order factor. An OF is required if the recombination lifetime varies with charge density (i.e., the effective order of the process is not 1). The OF is given by $(-S + 1)$ where S is the slope of $\log(\tau)$ vs $\log(Q)$ in Figure 5c.[46,47] We can make this calculation for the short and long lifetimes and total or above baseline charge (Table 1). If the implied recombination current is not physically reasonable, then the specific TPV decay is unlikely to be a measure of recombination in the cell. For example, for 60 s self-TEBBing at 1 sun V_{oc}, using the shorter lifetime (0.93 μs, Figure 5c) and the "charge above baseline" (89 nC/cm^2, Figure 3d) with an order factor of 4.4 (from Figure 5c), we calculate a recombination current of 22 mA/cm^2 (see Table 1, line 1). This value is reasonable given that the intensity of the LED bias light was equivalent to ∼1.2 suns. At the same intensity, the maximum J_{sc} after 60 s TEBBing is ∼26 mA/cm^2 (Figure 1c). The implication of an estimated recombination current of 22 mA/cm^2 at the 1 sun V_{oc} is that charge generation efficiency is not significantly reduced at V_{oc} relative to short circuit, if at all. In other words, charge generation from absorbed photons is not a function of internal electric field. We believe this is reasonable given the high dielectric and low exciton binding energies proposed for MAPI.

In Table 1, we give the recombination current calculation using other combinations of τ and charge and also for 10% bias light intensity. For example, the calculated recombination current for 60 s self-TEBBing, 10% sun, the short lifetime, and the charge above baseline is 2.6 mA/cm^2 (Table 1, line 5), quite close to 1/10 of the estimate at 1 sun. On the other hand, the J_{rec} calculated for the short lifetime, with the total capacitive charge, is 39 mA/cm^2 (line 3). Because this is ∼50% higher than the maximum possible, it is clearly not physically reasonable. The implication is thus that the charges held in the baseline capacitance do not participate in the fast recombination process.

Two additional conclusions can be drawn from Table 1. First, the recombination current at V_{oc} before and after self-TEBBing is similar. For example, the recombination currents at 5 and 60 s self-TEBBing, at both 1 and 10% sun are almost identical (lines 1 and 1a and 5 and 5a). This indicates that the increase in J_{sc} and V_{oc} after self-TEBBing is *not* due to an increase in charge generation efficiency in the bulk of the film. By extension, if the ferroelectric domain structure of the cell is involved in self-TEBBing, it is not by a simple increase in charge generation. Second, the last two lines of Table 1 show the recombination current calculated using the fast or slow TPV lifetime and the charge measured by charge extraction (40 μC/cm^2, Figure 2d). The implied recombination currents are 14 and 3 A/cm^2, respectively, which are both >100 times the maximum possible charge generation current. We can conclude that the charge measured by charge extraction does not contribute to the TPV decays shown in Figure 5 and is thus almost certainly not electronic in nature. It must instead be due to moving ions or reorienting dipoles.

It remains to discuss the assignment of the slower phase of the TPV decay. Lines 2 and 4 give the calculated J_{rec} using the longer TPV lifetime and the total or above baseline charge. The values, 11 and 6.9 mA/cm^2, respectively, are well below the measured photocurrent following 60 s self-TEBBing. All the other J_{rec} estimates using the longer lifetimes also give values that are smaller than the J_{sc} produced in the same condition (see Table 1 lines in italics). If we were to make the assumption that the slower TPV lifetime represents the main electron/hole recombination, we would have two issues. First, we would have to explain the fast decay by some other process. We give evidence against this possibility further below. Second, the low J_{rec} would imply that charge generation at V_{oc} is significantly less efficient than that at short circuit. Lacking other evidence to support this possibility, we assert that the slower lifetime does not correspond to the *predominant* channel of electron/hole recombination in the bulk of the device. The results do not rule out that the slow phase of the TPV results from a secondary recombination channel. However, this cannot be proven or disproven using Table 1. All possible sums of J_{rec} for one fast and one slow phase exceed the maximum possible recombination current (e.g., line 1 plus line 2 gives 29 mA/cm^2). However, the uncertainty in the calculation is probably larger than the difference. (We note that the statements in this paragraph are also true for J_{rec} values calculated with the integrated capacitance below the baseline, not included in the table for brevity.)

Modeling Double Exponential TPV Decays. To examine under what conditions the double exponential decay could represent two channels of recombination in the cell, we have looked for physically reasonable models of the cell that can recreate the TPV decays. In constructing a model, we have assumed that it is the presence of the mpTiO_2 that creates the double exponential decay. In some preliminary tests, we find that cells of the type FTO/sTiO_2/MAPI/SOT/Au show only single exponential TPV decays (Figure S6a, Supporting Information). The fact that the two TPV time constants keep the same ratio as V_{oc} changes indicates that there is a link between the sources of the two time constants. Thus, another possible model, where voltage is created and decays separately at the TiO_2/MAPI and MAPI/SOT interfaces, seems less likely. Figure 6a shows a possible model. Though this model looks similar to those used for DSSCs, we caution that the interpretations of the components are different. Also, the placement of the electrical components with respect to the physical components should be held as an open question. We intend this model to be a starting point for discussion, not as a final assignment. We also point out that this model does not concern the TEBBing effect. We could include a band edge offset variable to recreate the effect of TEBBing on V_{oc}, but this would not mimic the effect on FF or dark current, so we have not done so.

We can use the model in Figure 6a in two ways. For the first, we assume that the sTiO_2, mpTiO_2, and MAPI are not doped and that the SOT is highly doped, thus the cell has a p-i-n structure. In a p-i-n structure, the built in voltage (V_{bi}) drops more or less linearly across the intrinsic active region of the cell. The capacitance, C3 (Figure 6b), represents the geometrical capacitance between the FTO and SOT layers. The magnitude of C3 is dependent on the thickness and dielectric constants of the mpTiO_2 and MAPI layers. When light is absorbed by the MAPI, holes and electrons are created. Electrons drift toward the sTiO_2 layer under the influence of V_{bi}. Along the way, some of the electrons are injected into the mpTiO_2. Evidence suggests a significant fraction of the electrons could reach the sTiO_2 and be transferred to the TiO_2 at that point. The fraction of electrons injected into the mpTiO_2 may be dependent on the fabrication method used and may even vary with applied potential. For the p-i-n model, we assume that electrons injected into the sTiO_2 charge C3 directly, and Cμ1 is set to zero. Electrons from C3 recombine with holes via Rre1. In the p-i-n model, electrons injected into the mpTiO_2 create no

DOI: 10.1021/jacs.5b00761
J. Am. Chem. Soc. 2015, 137, 5087−5099

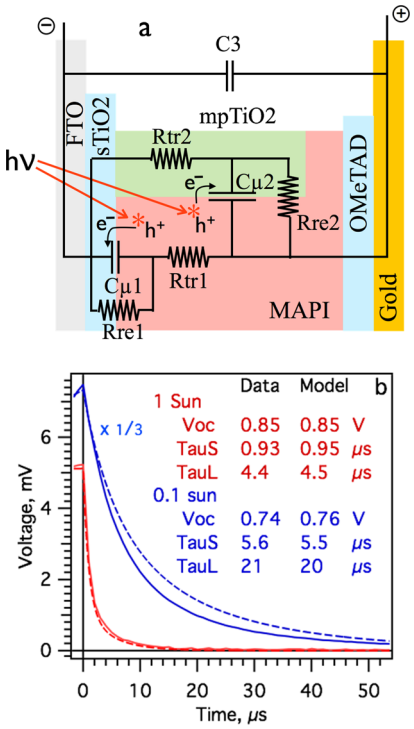

Figure 6. (a) Schematic electrical model of $mpTiO_2$/MAPI cell. (b) Measured and modeled TPV transients. Measured and modeled decays for 0.1 sun have been divided by 3 to improve clarity. Model data have been normalized up to match measured data at time zero, by 1.3 and 1.15 for 1 sun and 0.1 sun, respectively. Inset: table with measured and modeled V_{oc} and the short and long lifetimes from double exponential fits of the TPV decays.

significant electric field between the $mpTiO_2$ and the MAPI but change the trap occupancy and quasi-Fermi level in the $mpTiO_2$. Electrons in the $mpTiO_2$ are transported by drift to the $sTiO_2$ (Rtr2), or they can recombine with holes (Rre2). Transport is modeled with a charge density dependent mobility, and Rre2 is modeled using a charge density dependent lifetime, both as power laws. The exponents with respect to charge for both are 2.5, taken from Figure 5. For this simple model, we have neglected the transport of holes and the diffusion of electrons. More details of the model are given in the Supporting Information. Despite the obvious over-simplification, this model can reproduce the V_{oc}, the two TPV lifetimes, and their trends with bias light intensity (Figure 6b). In this model, the faster component of the TPV decay represents recombination of the excess electrons in C3 through Rre1. As this decay occurs, additional excess electrons flow to C3 by transport from Cμ2. This current decays with the time constant of recombination through Rre2. This simple model can also reproduce the TPV peak heights and magnitude of the two components at 1 sun. However, as we show in the next paragraph, this model is not unique; thus we will not draw any physical conclusions from it at this time.

Our preliminary data on planar MAPI cells (FTO/$sTiO_2$/MAPI/SOT/Au) indicates that the short lifetime in Figure 3 is a result of the $mpTiO_2$ layer (Figure S6a, Supporting Information). This would be consistent with the generally higher voltage reported for planar cells. We were unable to find parameter sets for the above model where-in the fast decay came from the $mpTiO_2$, presumably because a drift only model cannot move electrons from the $sTiO_2$ out to the $mpTiO_2$ to recombine. Thus, we have constructed a second model. For this model, we assume that the MAPI shields most of the built in potential to the edges of the MAPI layer. This could be due to accidental n or p doping during fabrication, movement of ions, or alignment of dipoles. We can model this case using Figure 6a by using Cμ1 to model the capacitance at the $sTiO_2$/MAPI interface, and by ignoring the effect of V_{bi} on the transport of electrons in and out of the $mpTiO_2$. We set the decay of electrons from the $mpTiO_2$ to be faster than that from $sTiO_2$. We use the difference in electrochemical potential between Cμ1 and Cμ2 to determine which way current is flowing. With relatively large values of Rtr1 and Rtr2 to semi-isolate the two systems, this model can reproduce the measured data as well as does the previous model (Figure S6b, Supporting Information). Further experimental evidence on the electric field inside the MAPI layer will be required before a choice can be made between these two models or others. Lastly, one might also be tempted to assign the slow component of the TPV decay to recombination directly from TiO_2 to SOT. However, the recombination lifetimes in solid state DSSCs, which also have $mpTiO_2$/SOT contact, are on the order of 1 ms, 100 times longer than the slow decay seen here.[40,41,48]

Other Possible Sources of Fast TPV Decays. In the above discussion and modeling, we have asserted that the fast component of the TPV decay represents the main loss of charge in the cell. However, before accepting this assignment we should examine the alternatives. The only way that the pulse can create a voltage signal is by causing a net separation of positive and negative charge along a vector normal to the cell contacts. The decay of the voltage corresponds to the decay of the net separation. However, the decay does not have to be recombination. There are (at least) three ways that the TPV pulse could establish a voltage that would decay by a mechanism different from recombination. These are as follows: (1) Illumination that is strongly absorbed on one side of the active layer can create charges that separate because of unequal mobility. In this case, equilibration of the charge distributions can cause decay of the photovoltage without recombination. (2) In the "bulk photovoltaic effect", the absorption of light in a non-centrosymmetric material can result in a net separation of charges along some directions in the crystal. The voltage can again decay by equilibration of the charge distributions without recombination. (3) A photo-"isomerization" effect can turn dipoles or shifts ionic charges rather than electronic charges. In this case, the photovoltage decay occurs by rotation or movement of atomic charges rather than recombination of electronic charge. For all three of these possibilities, we believe it is possible to show that they are not the source for the fast component of the TPV decays measured on our cells.

With respect to mechanism 1, the photovoltage decay occurs by charge transport. The hole and electron mobilities in MAPI are reported to be in the 2–20 $cm^2/(V\,s)$ range.[16,28,49] At the 1 sun V_{oc} (~0.85 V), there will remain a built in field of perhaps 0.3 V. Under this field, the transit time of electrons and holes across the film is only a few nanoseconds. Thus, any voltage decay that depends on charge transport rather than recombination should fall in the <20 ns time scale. Consistent with this, when using a 20 ns laser pulse, >80% of the voltage rise occurs within the pulse (Figure S5a, Supporting Information). The fast component of the TPV decay is 1 μs at 1 sun. This is at least 50 times longer than the apparent charge transport times, indicating that the fast TPV decay is not due to mechanism 1 in the previous paragraph. Further, the

DOI: 10.1021/jacs.5b00761
J. Am. Chem. Soc. 2015, 137, 5087–5099

optical density of our films at 650 nm is about 1. This means that only about twice as many photons are absorbed in the front half of the film. This absorption is a bit weak to cause a voltage signal by mechanism 1.

With regard to the bulk photovoltaic effect, we can ask whether there are enough photons in the pulse to create the observed voltage increase during the first 2 μs of the pulse. The bulk photovoltaic effect occurs when absorption of light directly creates a separation of electrons and holes. The separation is said to be limited to at most a few mean free paths. In Figure 3a, the first 2 μs of the pulse results in absorption of $\sim 4 \times 10^{10}$/cm^2 photons and creates a voltage increase of 4 mV. Using a relative dielectric constant of 20, the electron/hole separation per photon would have to be 10 nm.[50] Although this is probably too large, it might be possible. However, the argument from the proceeding paragraph holds here as well. Given the published values for the mobility, it should take only a few nanoseconds for these charges to re-equilibrate after the end of the pulse, instead of the 1 μs measured. With respect to mechanism 3, we assume that each absorbed photon can rotate at most one methylammonium (MA) dipole. The partial charge on the MA dipole is about 0.3q. During the first 2 μs of the pulse, rotation of $\sim 4 \times 10^{10}$ MA dipoles in the film volume (300 nm $\times$ 1 cm^2), again using a dielectric constant of 20, should give rise to a voltage signal of only ~0.2 mV. Although this is too small relative to the fast component of the TPV decay, it is similar to the magnitude of the slow phase, especially for the cell with the 5 s self-TEBBing time (Figure 5d).

Discussion of Error in Capacitance Calculation. The next two paragraphs discuss the possible errors in the calculation of the capacitance. There are two kinds of errors that might be present: those that change the absolute magnitude of the two capacitance curves (short and long self-TEBBed) and those that change the voltage shift between them. The measurement of dV/dt from the voltage transient appears unlikely to have significant error. The main source of error is our estimate of dQ/dt at V_{oc} from the SC photocurrent transients. Taking the 26 mA/cm^2 photocurrent after full TEBBing as ~100% internal photocurrent quantum efficiency (Figure 1c), we estimate the internal quantum efficiency at short circuit as ~45% for 5 s self-TEBBing and ~60% for 60 s self-TEBBing. The photocurrent transients in Figure 3b could be underestimating the amount of charge created by the pulse at V_{oc}. If so, the correct capacitance could be up to 2 times higher than we have calculated. This correction would have essentially no effect on the large difference between the charge measured by charge extraction and that measured by differential capacitance, one of our primary observations. The correction also would not remove the shift in the capacitance vs voltage curves in Figure 3c, though it could reduce it from 120 to 100 mV.

The second assumption we have made is that the charge generation efficiency does not decrease when moving from SC to OC. This assumption has turned out to be correct for both DSSCs and many types of polymer cells.[39,51,52] It turns out to give a self-consistent estimation of recombination flux using eq 1. However, it can only be proven by transient absorption experiments. If in fact charge generation efficiency is smaller at OC, then the dQ/dt values estimated from the J_{sc} transients are too large. The correct capacitance would be significantly smaller than that shown in Figure 3d. A self-consistent calculation with eq 1 would then probably require the total charge, instead of the charge above baseline.

CONCLUSIONS

We have demonstrated that in mpTiO$_2$/MAPI cells there are two kinds of extractable charge stored when the cell is held at V_{oc}: a capacitive electronic charge (~0.2 μC/cm^2) and another, much larger charge (40 μC/cm^2), which could be the result of dipole realignment or the effect of mobile ions. The capacitive charge is ~10 times smaller than that in mpTiO$_2$/dye/SOT cells with similar mpTiO$_2$ thickness. By measurement of the capacitive charge after different equilibration times at V_{oc}, we show that the J–V hysteresis in mpTiO$_2$/MAPI cells involves a change in internal potential gradients, most likely a shift in band offsets at the TiO$_2$/MAPI interface. In mpTiO$_2$/MAPI cells, the transient photovoltage decays are strongly double exponential with two time constants that differ by a factor of ~5, independent of bias light intensity. The fast decay (~1 μs at 1 sun) can be assigned to the predominant charge recombination pathway in the cell. The TPV results show that the V_{oc} hysteresis is not due to a change in recombination rate constant. Calculation of recombination flux at V_{oc} shows that the hysteresis is also not due to an increase in charge separation efficiency and that charge generation is not a function of applied bias. We also show that the J–V hysteresis is not a light driven effect but is caused by exposure to forward bias, light or dark.

In addition, we want to stress the complexity of the hysteresis displayed by these cells. As mentioned above, there seem to be two or three different processes visible in Figure 1c, occurring on the 0.5 to 20 s time scale. In addition, there is the ~1 ms time scale process shown in Figure S5e, Supporting Information. These results are consistent with the multiple processes measured on the 100 μs to seconds time scale in impedance studies. If the 1 and 5 μs TPV decays (at 1 sun) account for all of the electronic recombination in the cell, as seems likely from Table 1, then all these slower processes are chemical in nature. By "chemical", we mean they involve the movement of atoms (dipoles or ions) instead of, or in addition to, electrons. How to reconcile the simultaneous increase in dark current and increase in photocurrent in Figure 1c will require careful separation of the bulk changes and interface changes occurring during TEBBing.

ASSOCIATED CONTENT

Supporting Information

Additional J–V measurements, capacitive discharge current, time evolution of the J_{sc} and V_{oc} under illumination, comparison of charge extraction current in MAPI cells and DSSCs, photovoltage transients after short and long TEBBing times, capacitance vs voltage for additional cells, full TPV decays covering 0.05–2 suns, photovoltage transients as a function of pulse length, photovoltage transients for planar MAPI cells, and details of the electrical models. This material is available free of charge via the Internet at http://pubs.acs.org.

AUTHOR INFORMATION

Corresponding Author

*b.oregan@imperial.ac.uk

Notes

The authors declare no competing financial interest.

DOI: 10.1021/jacs.5b00761
J. Am. Chem. Soc. 2015, 137, 5087–5099

■ ACKNOWLEDGMENTS

This work was supported by the UK EPSRC Grants EP/I019278/1 and EP/M014797/1, the Spanish MINECO project CQT2013-47183R, and the Severo Ochoa Excellence Accreditation 2014.2018 (SEV-2013-0319). P. Barnes thanks the EPSRC for his fellowship (EP/J002305/1).

■ REFERENCES

(1) Kojima, A.; Teshima, K.; Shirai, Y.; Miyasaka, T. *J. Am. Chem. Soc.* **2009**, *131*, 6050.
(2) Wojciechowski, K.; Stranks, S. D.; Abate, A.; Sadoughi, G.; Sadhanala, A.; Kopidakis, N.; Rumbles, G.; Li, C.-Z.; Friend, R. H.; Jen, A. K.-Y.; Snaith, H. J. *ACS Nano* **2014**, *8*, 12701.
(3) Burschka, J.; Pellet, N.; Moon, S. J.; Humphry-Baker, R.; Gao, P.; Nazeeruddin, M. K.; Gratzel, M. *Nature* **2013**, *499*, 316.
(4) Jeon, N. J.; Noh, J. H.; Kim, Y. C.; Yang, W. S.; Ryu, S.; Il, S. S. *Nat. Mater.* **2014**, *13*, 897.
(5) Sanchez, R. S.; Gonzalez-Pedro, V.; Lee, J. W.; Park, N. G.; Kang, Y. S.; Mora-Sero, I.; Bisquert, J. *J. Phys. Chem. Lett.* **2014**, *5*, 2357.
(6) Bi, D. Q.; Yang, L.; Boschloo, G.; Hagfeldt, A.; Johansson, E. M. J. *J. Phys. Chem. Lett.* **2013**, *4*, 1532.
(7) Zhao, Y. X.; Nardes, A. M.; Zhu, K. *J. Phys. Chem. Lett.* **2014**, *5*, 490.
(8) Roiati, V.; Colella, S.; Lerario, G.; De Marco, L.; Rizzo, A.; Listorti, A.; Gigli, G. *Energy Environ. Sci.* **2014**, *7*, 1889.
(9) Guillen, E.; Ramos, F. J.; Anta, J. A.; Ahmad, S. *J. Phys. Chem. C* **2014**, *118*, 22913.
(10) Dualeh, A.; Moehl, T.; Tetreault, N.; Teuscher, J.; Gao, P.; Nazeeruddin, M. K.; Gratzel, M. *ACS Nano* **2014**, *8*, 362.
(11) Bergmann, V. W.; Weber, S. A. L.; Ramos, F. J.; Nazeeruddin, M. K.; Gratzel, M.; Li, D.; Domanski, A. L.; Lieberwirth, I.; Ahmad, S.; Berger, R. *Nat. Commun.* **2014**, *5*, No. 5001.
(12) Barnea-Nehoshtan, L.; Kirmayer, S.; Edri, E.; Hodes, G.; Cahen, D. *J. Phys. Chem. Lett.* **2014**, *5*, 2408.
(13) Wang, L. L.; McCleese, C.; Kovalsky, A.; Zhao, Y. X.; Burda, C. *J. Am. Chem. Soc.* **2014**, *136*, 12205.
(14) Somsongkul, V.; Lang, F.; Jeong, A. R.; Rusu, M.; Arunchaiya, M.; Dittrich, T. *Phys. Status Solidi RRL* **2014**, *8*, 763.
(15) Lee, J. W.; Lee, T. Y.; Yoo, P. J.; Gratzel, M.; Mhaisalkar, S.; Park, N. G. *J. Mater. Chem. A* **2014**, *2*, 9251.
(16) Wang, Q.; Shao, Y. C.; Xie, H. P.; Lyu, L.; Liu, X. L.; Gao, Y. L.; Huang, J. S. *Appl. Phys. Lett.* **2014**, *105*, No. 163508.
(17) Abate, A.; Saliba, M.; Hollman, D. J.; Stranks, S. D.; Wojciechowski, K.; Avolio, R.; Grancini, G.; Petrozza, A.; Snaith, H. J. *Nano Lett.* **2014**, *14*, 3247.
(18) Snaith, H. J.; Abate, A.; Ball, J. M.; Eperon, G. E.; Leijtens, T.; Noel, N. K.; Stranks, S. D.; Wang, J. T. W.; Wojciechowski, K.; Zhang, W. *J. Phys. Chem. Lett.* **2014**, *5*, 1511.
(19) Unger, E. L.; Hoke, E. T.; Bailie, C. D.; Nguyen, W. H.; Bowring, A. R.; Heumüller, T.; Christoforo, M. G.; McGehee, M. D. *Energy Environ. Sci.* **2014**, *7*, 3690.
(20) Gottesman, R.; Haltzi, E.; Gouda, L.; Tirosh, S.; Bouhadana, Y.; Zaban, A.; Mosconi, E.; de Angelis, F. *J. Phys. Chem. Lett.* **2014**, *5*, 2662.
(21) Kim, H. S.; Park, N. G. *J. Phys. Chem. Lett.* **2014**, *5*, 2927.
(22) Frost, J. M.; Butler, K. T.; Walsh, A. *APL Mater.* **2014**, *2*, No. 081506.
(23) Jeon, N. J.; Lee, J.; Noh, J. H.; Nazeeruddin, M. K.; Gratzel, M.; Seok, S. I. *J. Am. Chem. Soc.* **2013**, *135*, 19087.
(24) Malinkiewicz, O.; Roldan-Carmona, C.; Soriano, A.; Bandiello, E.; Camacho, L.; Nazeeruddin, M. K.; Bolink, H. J. *Adv. Energy Mater.* **2014**, *4*, No. 1400345.
(25) Kutes, Y.; Ye, L. H.; Zhou, Y. Y.; Pang, S. P.; Huey, B. D.; Padture, N. P. *J. Phys. Chem. Lett.* **2014**, *5*, 3335.
(26) Tress, W.; Marinova, N.; Moehl, T.; Zakeeruddin, S. M.; Nazeeruddin, M. K.; Gratzel, M. *Energy Environ. Sci.* **2015**, *8*, 995.
(27) Xiao, Z.; Yuan, Y.; Shao, Y.; Wang, C.; Dong, Q.; Cheng, B.; Shamar, P.; Gruverman, A.; Huang, J. *Nat. Mater.* **2014**, *14*, 193.
(28) Savenije, T. J.; Ponseca, C. S.; Kunneman, L.; Abdellah, M.; Zheng, K. B.; Tian, Y. X.; Zhu, Q. S.; Canton, S. E.; Scheblykin, I. G.; Pullerits, T.; Yartsev, A.; Sundstrom, V. *J. Phys. Chem. Lett.* **2014**, *5*, 2189.
(29) Lee, M. M.; Teuscher, J.; Miyasaka, T.; Murakami, T. N.; Snaith, H. J. *Science* **2012**, *338*, 643.
(30) Kim, H. S.; Lee, C. R.; Im, J. H.; Lee, K. B.; Moehl, T.; Marchioro, A.; Moon, S. J.; Humphry-Baker, R.; Yum, J. H.; Moser, J. E.; Gratzel, M.; Park, N. G. *Sci. Rep.* **2012**, *2*, No. 591.
(31) Xu, W. W.; Kershaw, R.; Dwight, K.; Wold, A. *Mater. Res. Bull.* **1990**, *25*, 1385.
(32) O'Regan, B.; Xiaoe, L.; Ghaddar, T. *Energy Environ. Sci.* **2012**, *5*, 7203.
(33) O'Regan, B. C.; Scully, S.; Mayer, A. C.; Palomares, E.; Durrant, J. *J. Phys. Chem. B* **2005**, *109*, 4616.
(34) Barnes, P. R. F.; Miettunen, K.; Li, X. E.; Anderson, A. Y.; Bessho, T.; Gratzel, M.; O'Regan, B. C. *Adv. Mater.* **2013**, *25*, 1881.
(35) Stranks, S. D.; Eperon, G. E.; Grancini, G.; Menelaou, C.; Alcocer, M. J. P.; Leijtens, T.; Herz, L. M.; Petrozza, A.; Snaith, H. J. *Science* **2013**, *342*, 341.
(36) Yamada, Y.; Nakamura, T.; Endo, M.; Wakamiya, A.; Kanemitsu, Y. *J. Am. Chem. Soc.* **2014**, *136*, 11610.
(37) Duffy, N. W.; Peter, L. M.; Rajapakse, R. M. G.; Wijayantha, K. G. U. *Electrochem. Commun.* **2000**, *2*, 658.
(38) Shuttle, C. G.; Maurano, A.; Hamilton, R.; O'Regan, B.; de Mello, J. C.; Durrant, J. R. *Appl. Phys. Lett.* **2008**, *93*, No. 183501.
(39) Anderson, A. Y.; Barnes, P. R. F.; Durrant, J. R.; O'Regan, B. C. *J. Phys. Chem. C* **2010**, *114*, 1953.
(40) O'Regan, B. C.; Shuttle, C.; Handa, S.; Koops, S.; Durrant, J. R. *Org. Photovoltaics* **2006**, *6334* (VII), No. 633406.
(41) Chen, P.; Yum, J. H.; De Angelis, F.; Mosconi, E.; Fantacci, S.; Moon, S. J.; Baker, R. H.; Ko, J.; Nazeeruddin, M. K.; Gratzel, M. *Nano Lett.* **2009**, *9*, 2487.
(42) Cai, N.; Moon, S. J.; Cevey-Ha, L.; Moehl, T.; Humphry-Baker, R.; Wang, P.; Zakeeruddin, S. M.; Gratzel, M. *Nano Lett.* **2011**, *11*, 1452.
(43) Koops, S. E.; O'Regan, B. C.; Barnes, P. R. F.; Durrant, J. R. *J. Am. Chem. Soc.* **2009**, *131*, 4808.
(44) Listorti, A.; Creager, C.; Sommeling, P.; Kroon, J.; Palomares, E.; Fornelli, A.; Breen, B.; Barnes, P. R. F.; Durrant, J. R.; Law, C.; O'Regan, B. *Energy Environ. Sci.* **2011**, *4*, 3494.
(45) Roiati, V.; Mosconi, E.; Listorti, A.; Colella, S.; Gigli, G.; De Angelis, F. *Nano Lett.* **2014**, *14*, 2168.
(46) O'Regan, B. C.; Durrant, J. R.; Sommeling, P. M.; Bakker, N. J. *J. Phys. Chem. C* **2007**, *111*, 14001.
(47) Bisquert, J. *J. Phys. Chem. B* **2004**, *108*, 2323.
(48) Dualeh, A.; De Angelis, F.; Fantacci, S.; Moehl, T.; Yi, C. Y.; Kessler, F.; Baranoff, E.; Nazeeruddin, M. K.; Gratzel, M. *J. Phys. Chem. C* **2012**, *116*, 1572.
(49) Leijtens, T.; Stranks, S. D.; Eperon, G. E.; Lindblad, R.; Johansson, E. M. J.; McPherson, I. J.; Rensmo, H.; Ball, J. M.; Lee, M. M.; Snaith, H. J. *ACS Nano* **2014**, *8*, 7147.
(50) Brivio, F.; Walker, A. B.; Walsh, A. *APL Mater.* **2013**, *1*, No. 042111.
(51) Jamieson, F. C.; Agostinelli, T.; Azimi, H.; Nelson, J.; Durrant, J. R. *J. Phys. Chem. Lett.* **2010**, *1*, 3306.
(52) Haque, S. A.; Tachibana, Y.; Willis, R. L.; Moser, J. E.; Grätzel, M.; Klug, D. R.; Durrant, J. R. *J. Phys. Chem. B* **2000**, *104*, 538.

DOI: 10.1021/jacs.5b00761
J. Am. Chem. Soc. 2015, 137, 5087−5099